Biochimica et Biophysica Acta 1788 (2009) 1024–1032

Contents lists available at ScienceDirect

Biochimica et Biophysica Acta

journal homepage: www.elsevier.com/locate/bbamem

Ion binding properties and structure stability of the NaK channel

Rong Shen, Wanlin Guo *

Institute of Nano Science, Nanjing University of Aeronautics and Astronautics, Nanjing 210016, China

ARTICLE INFO

Article history:
Received 27 August 2008
Received in revised form 9 January 2009
Accepted 13 January 2009
Available online 6 February 2009

Keywords:
NaK channel
Molecular dynamics
Ion distribution
Ion solvation

ABSTRACT

Ion distribution in the selectivity filter and ion–water and ion–protein interactions of NaK channel are systematically investigated by all-atom molecular dynamics simulations, with the tetramer channel protein being embedded in a solvated phospholipid bilayer. Analysis of the simulation results indicates that K^+ ions prefer to bind within the sites formed by two adjacent planes of oxygen atoms from the selectivity filter, while Na^+ ions are inclined to bind to a single plane of four oxygen atoms. At the same time, both K^+ and Na^+ ions can diffuse in the vestibule, accompanying with movements of the water molecules confined in a complex formed by the vestibule together with four small grottos connecting to it. As a result, K^+ ions show a wide range of coordination numbers (6–8), while Na^+ ions display a constant coordination number of ~6 in the selectivity filter, which may result in the loss of selectivity of NaK. It is also found that a Ca^{2+} can bind at the extracellular site as reported in the crystal structure in a partially hydrated state, or at a higher site in a full hydration state. Furthermore, the carbonyl group of Asp66 can reorient to point towards the center pore when an ion exists in the vestibule, while that of Gly65 always aligns tangentially to the channel axis, as in the crystallographic structures.

1. Introduction

The recently determined atomic structure of the NaK channel from *Bacillus cereus*, with properties of Na^+ and K^+ permeability and Ca^{2+} blockage, is the first structure of cation channels without high selectivity to K^+ ion [1]. The NaK channel shows remarkable similarity in the selectivity filter sequence with that of most cyclic nucleotide-gated (CNG) channels and exhibits similar ion permeation and external Ca^{2+} blocking properties, and it may resemble that of a CNG channel center pore structurally [2–4]. Therefore, investigation of the NaK channel will provide us an essential understanding of the underlying mechanisms governing ion conduction and Ca^{2+} blockage of the CNG channels.

The overall amino acid sequence and general architecture of NaK are very similar to that of the KcsA K^+ channel from *Streptomyces lividans* [5]. It is a tetramer with four identical subunits surrounding symmetrically around a central pore. Each subunit has two transmembrane helices connected by a pore loop which contains a pore helix and a selectivity filter with a signature sequence $_{63}$TVGDG$_{67}$. Comparing with the signature sequence $_{75}$TVGYG$_{79}$ in the selectivity filter of KcsA, NaK has a negatively charged residue Asp66 at the position equivalent to Tyr78 in KcsA, which causes a significant structural difference between NaK and KcsA in the selectivity filter. The carbonyl groups from $_{65}$GDG$_{67}$ residues of NaK adopt different conformations comparing with those from $_{77}$GYG$_{79}$ residues of KcsA (Fig. 1A and B). The Gly65 and Asp66, instead of pointing their backbone carbonyl oxygen atoms towards the center of the ion conduction pathway as Gly77 and Tyr78 in KcsA, are arranged with their carbonyl groups tangential to the pathway. Besides, the C_α atom of Asp66 is directed away from the ion conduction pore. These result in a bulging of the selectivity filter and form a vestibule in the region corresponding to the first two binding sites in the selectivity filter of KcsA. Four water grottos are found to connect to the vestibule, which form a vestibule–grottos complex in a plane perpendicular to the ion conducting pore (Fig. 1C and D) (R. Shen, W. L. Guo, and W. Y. Zhong, unpublished data). Gly65 and Asp66 residues from two adjacent filter loops form a narrow junction between the vestibule and grotto. Molecular dynamics (MD) simulations showed that each grotto could accommodate one water molecule optimally, and water molecules can be supplied from the extracellular solution into the grottos if there is initially no water molecule in the grottos. Exchange of water molecules between the vestibule and the grottos was also demonstrated (R. Shen, W. L. Guo, and W. Y. Zhong, unpublished data). High-resolution structures of KcsA under high and low K^+ concentrations revealed that there were one and three water molecules per subunit buried behind the selectivity filter respectively, bridging the interactions between residues in the selectivity filter and the remainder of the protein [6]. However their motions are limited and they do not exchange with water molecules in the filter or in the extracellular solution [7].

Occupancy and distribution of ions in the selectivity filter are essential to ion conduction properties and structure stability of the selectivity filter [6,8]. In the KcsA K^+ channel, the selectivity filter forms four potential ion binding sites referred to as S1–S4 from

* Corresponding author. Tel.: +86 25 84891896; fax: +86 25 84895827.
E-mail address: wlguo@nuaa.edu.cn (W. Guo).

0005-2736/$ – see front matter © 2009 Elsevier B.V. All rights reserved.
doi:10.1016/j.bbamem.2009.01.008

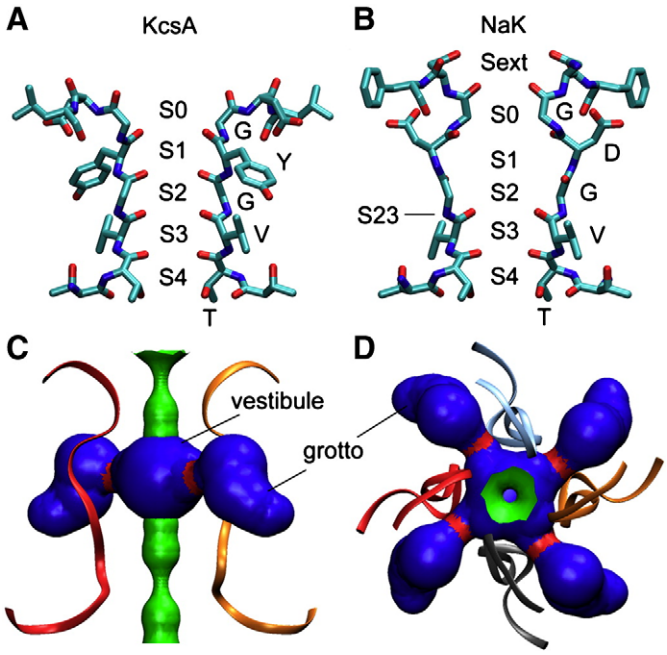

Fig. 1. Comparison of the selectivity filters of NaK and KcsA. (A) The selectivity filter of KcsA. (B) The selectivity filter of NaK. For convenience, we define all the possible sites (S0–S4) by the equivalent sites of a K^+ channel, site Sext is defined according to the NaK crystal structure, and an additional Na^+ specific site S23 between sites S2 and S3 is assigned. (C) Side view of the vestibule with two grottos connecting to it. (D) Top view of the vestibule–grottos complex. The red belts between the grottos and vestibule show the narrow necks with radius < 1.15 Å. For clarity, only two subunits are shown in (A, B, C).

extracellular to intracellular (Fig. 1A). Through a combination of electrophysiological, structural, and computational analyses, it is suggested that the KcsA K^+ channel prefers to contain two K^+ ions in the selectivity filter separated by one water molecule, and there exist mainly two alternative configurations of ions and water molecules in the selectivity filter, one with ions at sites S1 and S3 and water molecules at sites S2 and S4 (1, 3 configuration), and the other with ions at sites S2 and S4 and water molecules at sites S1 and S3 (2, 4 configuration) [8–11]. In contrast, electron density maps showed that the NaK channel created two potential ion binding sites at the intracellular entrance to the selectivity filter equivalent to sites S3 and S4 of KcsA, while forming a vestibule to replace the two upper ion binding sites corresponding to sites S1 and S2 of KcsA (Fig. 1A and B). Weak electron density was observed in the vestibule of NaK structure. It is suggested that the vestibule could accommodate a single ion with low occupancy and the ion could diffuse but not bind specifically in the vestibule [1]. Furthermore, K^+ ions are necessary to stabilize the selectivity filter of KcsA, the absence of K^+ ions [12] or binding of Na^+ ions [7,13,14] in the selectivity filter will distort the KcsA filter, whereas the Na^+ and K^+ complex structures of NaK revealed no apparent structural and ion distribution differences in the selectivity filter [1].

The NaK channel exhibits overall similarities and local differences in the amino acid sequence with KcsA and owns specific ion selectivity and permeation properties [1]. Based on the crystallographic structure of the NaK channel, Noskov and Roux [15] performed all-atom free energy perturbation molecular dynamics (FEP/MD) simulations and confirmed that the binding sites do not yield a large selectivity for K^+ in NaK compared to KcsA; the site S2, which is the most K^+-selective binding site in KcsA (~5 kcal/mol) [14], even exhibits a slight selectivity for Na^+ by up to −0.9 kcal/mol and −1.1 kcal/mol with the CHARMM27 [16] and AMBER [17] force fields, respectively. They attributed the loss of selectivity mainly to the increase in partial ion hydration. In a recent all-atom MD study of the NaK channel, Fowler et al. [18] investigated the selectivity of NaK by calculating the average number of coordinating ligands around the K^+ and Na^+ ions bound at either S2 or S4, then, they overlaid these data on the selectivity free energy contours, derived by population analysis of hydrated cations, from Bostick and Brooks III [19] and predicted that sites S2 and S4 are either not selective or are slightly selective for Na^+, as the coordination number of each bound ion is broadly similar to that of the ion in bulk water [19]. However, they found that the average hydration number of an ion at site S2 is either greater or smaller in NaK compared to KcsA, depending on the force field used, and predicted that the lack of selectivity of the NaK channel resulted from a reduction in the coordination number of the ions. Also, Vora et al. [20] studied the conduction of K^+ and Na^+ ions through a modified model of NaK, with M0 helix removed and the radii of the intracellular gate and the selectivity filter increased, using both Brownian and molecular dynamics, and found that the NaK channel indeed conducts both K^+ and Na^+ ions with a slightly higher permeability for the former. Although both experiments and theoretical calculations show that the NaK channel is nonselective, why the differences in the relative free energies of the ions at those binding sites are annihilated such that NaK is nonselective, and why and how both K^+ and Na^+ ions are able to obtain bulk-like coordination numbers remain elusive. In this paper we perform extensive molecular dynamics simulations of the NaK channel, embedded in a solvated phospholipid bilayer, with pure K^+ or Na^+ ions lining in the pore to study the dynamical properties of ions and water molecules in the selectivity filter, and the ion-filter and ion–water interactions. It is shown that both of the ions can diffuse in the vestibule and be hydrated by additional water molecules coming out from four small grottos connecting with the vestibule, and Na^+ ions take different binding sites in the filter than K^+ ions. These properties result in the achievement of favorable coordination states for both K^+ and Na^+ ions without causing major structural changes to the selectivity filter, which may significantly reduce the K^+ selectivity of NaK as suggested by previous MD studies [14,15,18,19].

2. Methods

2.1. Modeling

Two crystal structures of the NaK channel from *Bacillus cereus*, in both the Na^+- and K^+-bound states, were obtained recently [1]. In the present work, the monomer A from the K^+ complex structure of NaK (PDB ID 2AHZ) is used to build the basic atomic system (Fig. 2). Residues 106–110 at the C-terminus, which were not presented in the crystal structure, are omitted. The coordinates of the missing atoms of residue Met1 and protein hydrogen atoms are constructed using the PSFGEN plugin of VMD [21]. The side-chain of His96 is constructed in a neutral state, with its δ nitrogen being protonated to form a hydrogen bond with the carbonyl group of Leu98. The rest of the titratable residues are in their default titration state. A pre-equilibrated and pre-hydrated dimyristoylphosphatidylcholine (DMPC) lipid bilayer is used to build a 76 Å by 76 Å membrane, into which the NaK tetramer is embedded, by aid of the MEMBRANE plugin of VMD as shown in [22,23]. The membrane is centered at the Cartesian origin with its normal axis in *Z* direction. The protein is then inserted into the membrane with the pore along the *Z* axis, and the locations of Tyr42 and Trp19 are used to adjust the position of the protein along the *Z* axis. Lipids and water molecules overlapping with the protein are removed. Two water molecules and three K^+ ions are added into the pore as in configuration C13 as listed in Table 1. 38 water molecules are repositioned into the cavity from the bulk solution [24], and one water molecule is placed in each grotto as guided by the extensive simulations (R. Shen, W. L. Guo, and W. Y. Zhong, unpublished data). 19 Ca^{2+}, 2 K^+, and 55 Cl^- ions are inserted to preserve the electrically neutral of the whole system, one of the Ca^{2+} ions is then repositioned to site Sext. The final system contains totally 51,542 atoms, including

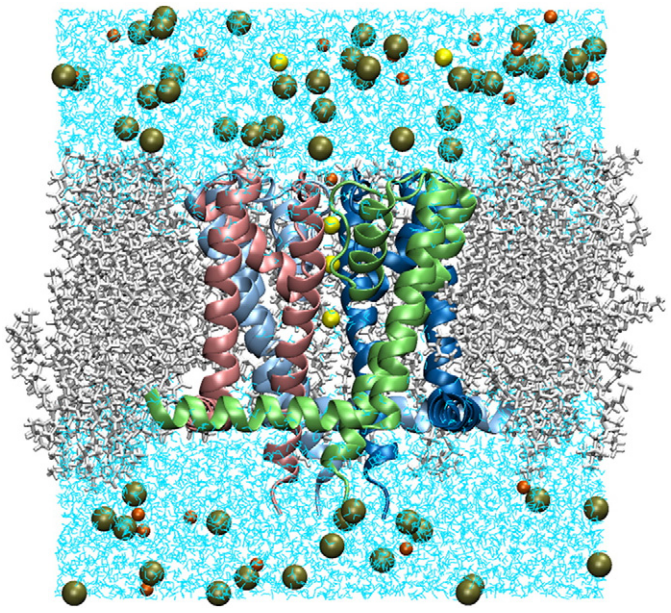

Fig. 2. Schematic representation of the atomic model of the basic NaK channel in its K^+–bound state embedded in a fully hydrated DMPC membrane. The four NaK subunits are shown in different colored ribbons, with three K^+ ions inside the pore and an Ca^{2+} ion binding at the extracellular entrance to the pore. The lipid molecules are shown in white sticks, and some of them are removed for clarity. Water molecules are represented in cyan lines. K^+, Ca^{2+} and Cl^- ions are shown in yellow, orange and tan spheres, respectively.

6900 protein atoms, 127 DMPC lipid molecules (67 and 60 in the extracellular and intracellular sides, respectively) with 14,986 atoms, 29,577 water atoms, 3 K^+ in the pore, and 19 Ca^{2+}, 2 K^+, and 55 Cl^- ions in the bulk solution.

2.2. Simulation protocols

The basic system is initially minimized for 5000 steps followed by a 200 ps equilibration period with the protein and ions in the pore being fixed to fill the gap between the protein and the lipids. The final structure is used to construct all of the rest configurations listed in Table 1. Then all of the systems are equilibrated for 800 ps with gradually decreasing harmonic restraints being applied to the protein and the ions in the pore. During this process, each of the Asp66–Tyr55 hydrogen bonds is restrained with a force constant of 3 kcal mol^{-1} $Å^{-2}$. In addition, harmonic restraints (with force constant of 2 kcal mol^{-1} $Å^{-2}$) are applied to oxygen atoms of the four water molecules in the grottos during these two equilibration periods. Then, the systems are simulated for additional 3 ns with no restraints.

All molecular dynamics simulations are performed with the program NAMD [25], the CHARMM27 force field for protein and phospholipids [16], and the TIP3P model for water [26]. Multiple sets of the Lennard–Jones parameters for K^+ and Na^+ ions are used to yield reasonable solvation free energies in bulk water and liquid N-methylacetamide [27]. Periodic boundary conditions are applied in all directions. The electrostatic interactions are calculated with no truncation using the particle mesh Ewald (PME) method [28] with a grid density of at least 1 $Å^{-3}$. Smooth (8–10 Å) switching off is applied for the van der Waals interactions. The time steps in all the molecular dynamics calculations are set at 1 fs. All simulations were performed in the NPT ensemble, the Langevin dynamics is employed to control the temperature at constant 310 K, and the Nosé-Hoover Langevin piston method [29,30] is used to maintain the pressure at 1 atm.

One-dimensional potential mean force (PMF) for the Ca^{2+} ion transition is calculated using umbrella sampling simulations [31]. The initial structure is the last frame of the MD simulation with K^+ ions in configuration C13. During umbrella sampling simulations, biasing harmonic potentials with a force constant of 20 kcal/mol are applied to the z coordinates of the Ca^{2+} ion (varying from 17.0 to 21.0 with 0.5 Å increments). After the energy minimization, each simulation is equilibrated for 100 ps prior to 400 ps of trajectory generation for analysis. The results are then unbiased and combined using the weighted histogram analysis method (WHAM) [32], with a bin width of 0.1 Å and a tolerance of 0.001 kcal/mol.

3. Results and discussion

3.1. Structural and dynamical properties

To characterize the influence of species and initial configuration of the ions in the pore on the conformational stability of the protein, we measured the average root mean square deviations (RMSDs) of backbone atoms of the entire tetramer and the selectivity filter from the crystal structure used to initiate the simulations (Table 1), and no significant deformation is observed. The backbone RMSDs of the protein are all less than 1.6 Å. In general, the backbone RMSD of the selectivity filter is less than that of the entire tetramer in the same system, while in the simulations with K^+ ions in configuration C24 and with Na^+ ions in configurations C14 and C24, the backbone RMSD of the selectivity filter is a little higher than that of the entire tetramer, and is highest in the Na^+ simulation with initial configuration C14. A closer examination of the selectivity filter reveals that the Ca^{2+} ion binding at the extracellular entrance to the pore departs from the site Sext during the simulation and induces the distortion of the filter (Fig. 3). It is also shown that simulations with K^+ or Na^+ ion at site S3 or S23 have lower backbone RMSDs of the selectivity filter than others.

Table 1
Summary of simulations

Sites	Initial configuration					Z (Å)
	C13	C14	C23	C24	C34	
Sext	Ca^{2+}	Ca^{2+}	Ca^{2+}	Ca^{2+}	Ca^{2+}	17.8
S0			w	w	w	14.7
S1	+	+	w	w	w	11.3
S2	w	w	+	+	w	8.4
S3	+	w	+	w	+	5.6
S4	w	+	w	+	+	2.6
Cavity	+	+	+	+	+	−2.5
Backbone RMSD for protein (Å)	1.28 ± 0.14 (1.58 ± 0.06)	1.36 ± 0.08 (1.37 ± 0.08)	1.44 ± 0.07 (1.40 ± 0.07)	1.42 ± 0.08 (1.28 ± 0.04)	1.46 ± 0.06 (1.33 ± 0.06)	
Backbone RMSD for filter (Å)	1.12 ± 0.10 (1.46 ± 0.14)	1.21 ± 0.11 (1.61 ± 0.10)	1.14 ± 0.12 (1.14 ± 0.09)	1.53 ± 0.12 (1.37 ± 0.12)	1.08 ± 0.11 (1.20 ± 0.09)	

Different initial configurations of ions (pure K^+ or Na^+) and water molecules within the pore, each site is occupied by an ion ("+") or a water molecule ("w"). RMSDs (mean ± s.d.) of backbone atoms of the protein and the selectivity filter from the crystal structure were averaged over the final 2 ns in each simulation, RMSDs in parentheses were for the simulations with Na^+ ions in the channel.

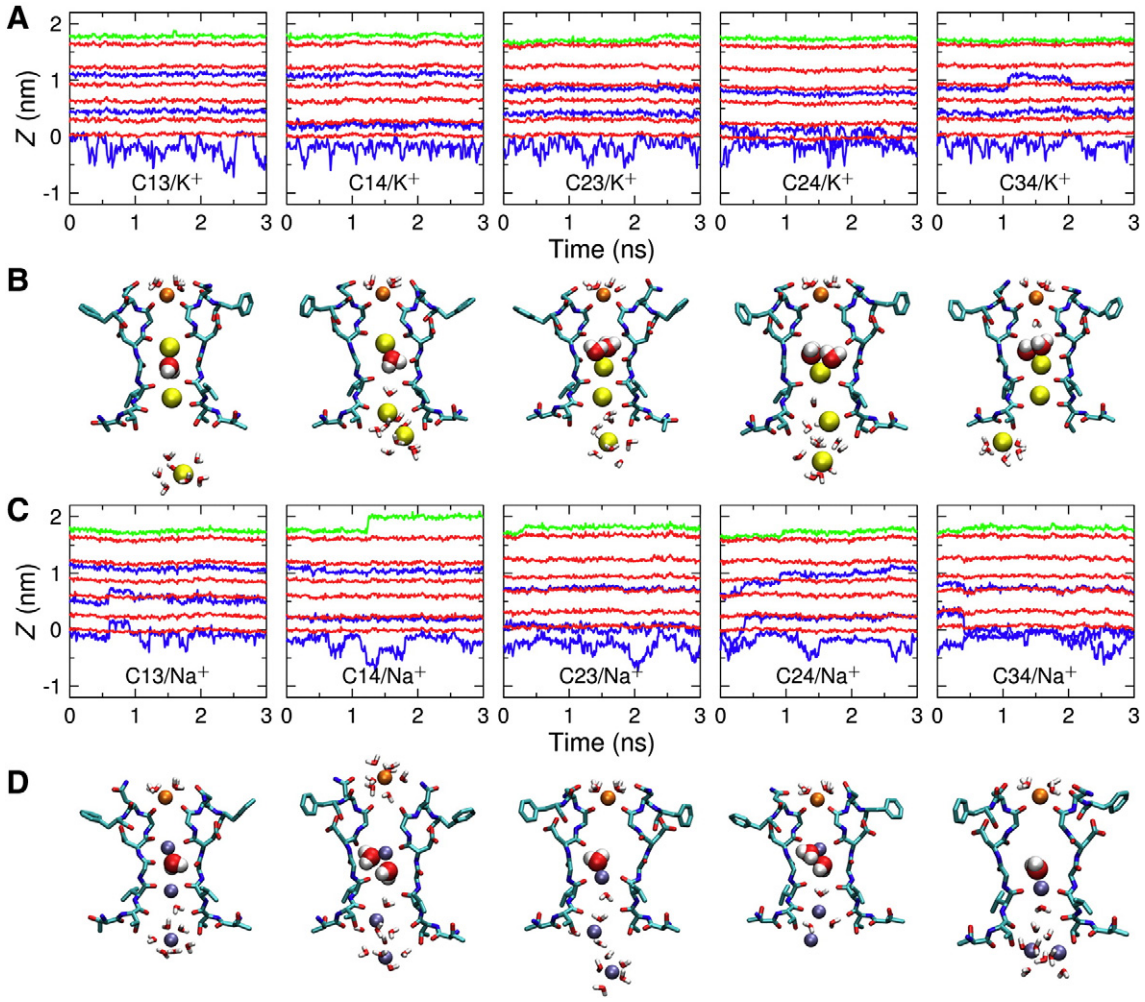

Fig. 3. Dynamic trajectories and final snapshots of ions in the pore. The *Z* trajectories of (A) K^+ ions and (C) Na^+ ions (blue), together with that of Ca^{2+} ion (green) and the oxygen atoms of the selectivity filter (red) in each simulation. (B) and (D) are final configurations of the ions and water molecules in the selectivity filter in the corresponding simulations presented in (A) and (C), respectively.

3.2. Dynamic transitions of ions and water molecules in the selectivity filter

Different behaviors of K^+ and Na^+ ions in the pore are studied by the time evolution of the *Z* trajectories of the ions (Fig. 3). For convenience, we use the case of C13/K^+ to represent the simulations with K^+ ions (K1, K2 and K3, numbered from the extracellular to intracellular sides) in configuration C13 initially. The same K^+ ion numbers are used for all the rest simulations.

Concerted transitions of K^+ ions and water molecules in a single file along the filter observed in previous MD simulations of KcsA [7,13,24], Kir6.2 [33], and NaK [18] are not observed in the present simulations of the NaK channel. In simulations with initial K^+ configurations of C13 and C23, the K^+ ions in the selectivity filter remain roughly near their initial positions throughout the periods of the simulations. In simulation C14/K^+, there is an initial relaxation from the starting configuration, the second ion, K2, displaces from the center of site S4 towards site S3, but no further motion of the ions can be seen. In contrast, the C14 configuration with two ions separated by two water molecules is not a stable state in KcsA, as it can convert rapidly into the C13 configuration [24]. In simulation C24/K^+, the K2 ion does not bind stably at site S4 as that in simulation C14/K^+, but diffuses in the cavity near to the bottom of the S4 site. The difference may be attributed to the stronger electrostatic ion–ion repulsion in C24 than in C14. In simulation C34/K^+, the ions at sites S3 and S4 have already transferred to sites S2 and S3, respectively, at the restraint equilibration period before the unrestrained simulation started. Comparing with C23/K^+, K^+ ion diffusion in the vestibule accompanying with the movement of water molecules in the vestibule–grottos complex is observed in C34/K^+. It is interesting to note that when the first K^+ ion, K1, transfers from site S2 to site S1, one of the two coordinating water molecules leaves the vestibule for one of the grottos. The C13-like intermediate configuration can last for about 1 ns and then converts to C23-like configuration when one water molecule from the grotto enters the vestibule to hydrate the K1 ion there. As can be seen from Fig. 3, the C_α atom of Gly67 is directed inwards and its carbonyl oxygen atom points towards the center pore as reported by Fowler [18], which causes the selectivity filter to shrink at the extracellular side, and site S0 becomes too narrow to accommodate a water molecule. We used to carry out C13-like simulations with an additional water molecule binding at site S0 initially, and found that the water molecule entered one of the grottos rapidly during the equilibration period with progressively decreasing restraint on its oxygen atom. Furthermore, analysis of the *Z* trajectories of the Ca^{2+} ion binding at site Sext reveals that the Ca^{2+} ion will displace outside a little if the water molecule departs from site S0.

As shown in Fig.3, Na^+ ions do not interact with the carbonyl oxygen atoms of the selectivity filter in the same way as K^+ ions. The K^+ ion tends to bind at the center of a cage of eight carbonyl oxygen atoms, while the Na^+ ion favors to bind at the center of four in-plane carbonyl oxygen atoms of the filter. It is in accord with previous MD

studies of the NaK channel. Noskov and Roux [15] reported that the Na^+ ion bound at site S3 of NaK can fluctuate near the top and bottom edges of the carbonyl cage. Vora et al. [20] obtained similar results that Na^+ ions are preferentially coordinated by single planes of carbonyl oxygens when they are forced to move through the selectivity filter. Such difference was also found in MD simulations of KcsA [7] and ab initio geometry optimized structures of a complex, which consists of an ion (K^+ or Na^+) bound in a reduced model of the binding site S2 of KcsA [34]. Our simulations with Na^+ ions in the pore reveal that Na^+ ion has a special preference to sit at site S23 to be in tight interactions with the four carbonyl oxygen atoms from Val64 and two water molecules above and below it. Ion diffusion in the vestibule is also observed in simulation C24/Na^+. With a start of C24/Na^+, the first ion, Na1, remains at site S2, while the ion Na2 at site S4 tends to run out to the cavity. After ~0.3 ns, Na2 re-enters the filter and occupies site S34 during the rest period of the simulation. Subsequently, Na1 moves towards site S1 and rests at site S1 during the last 2 ns of the simulation. Diffusion of Na1 in the vestibule is also accompanied by up to four water molecules. As shown in Fig. 4, unlike K^+ ions which can bind well within the defined binding sites S1–S4, Na^+ ions prefer to dwell between two binding sites except at site S1, which may be attributed to the electrostatic repulsion between the Ca^{2+} and Na1 ions. An additional preferential binding site is observed for both K^+ and Na^+ ions just beneath the selectivity filter, ions at this position can be stabilized by the side-chain oxygen atoms of residues Thr63.

An extracellular Ca^{2+} binding site was found in the NaK channel [1], and it is formed by the backbone carbonyl of Gly67. Alam et al. [3] suggested that Ca^{2+} binding to the extracellular entrance to the selectivity filter could stabilize the local structure, in addition to block monovalent cation conducting through the pore. Analysis of the trajectories shows that a Ca^{2+} ion can stay stably at site Sext in a partial hydration state, and carboxylate group of Asn68 also participate in binding the Ca^{2+} ion by interacting with water molecules surrounding it. It is also found through the simulation C14/Na^+ that the Ca^{2+} ion can bind at a higher site, Sadd as shown by Fig. 3C and D, which has not been detected in the crystal structure of NaK. The Ca^{2+} ion at site Sext is coordinated by 4 water molecules and four carbonyls from residues Gly67 precisely, whereas the Ca^{2+} ion at site Sadd is almost fully hydrated by ~7 water molecules as summarized in Table 2. This alternate Ca^{2+} binding position may suggest a new mechanism for the extracellular Ca^{2+} blocking process. As the protein forms an electronegative environment at the extracellular entryway to the selectivity filter, a hydrated Ca^{2+} ion in external solution can be attracted towards the entryway. The carboxylate groups of the side-chains of the four Asn68 residues pointing directly into the solution; together with the four carbonyls of Gly67 residues stabilize the almost fully hydrated Ca^{2+} ion at site Sadd. Then, when the Ca^{2+} hydration complex moves further towards site Sext through electrostatic attraction, the four carbonyl oxygen atoms from Gly67 residues replace ~3 of the hydrating water molecules, and the side-chains of Asn68 residues reorient accordingly to stabilize the half-dehydrated Ca^{2+} ion. Therefore, the side-chains of Asn68, the carbonyls of Gly67 and hydrating water molecules make contribution in conveying the Ca^{2+} ion from Sadd toward Sext and stabilizing it at the extracellular entryway. Fig. 5 shows the free energy profile as a function of the position of the Ca^{2+} ion. The Ca^{2+} ion can transit easily from site Sadd to Sext with a small energy barrier around 1.5 kcal/mol, while there exists a large free energy barrier up to ~4 kcal/mol to the transition from site Sext to Sadd. So the Ca^{2+} ion can bind stably at site Sext as reported in the experiment. Additionally, MD simulations show that K^+ and Na^+ cannot bind at sites Sext and Sadd as stably as Ca^{2+} and they will depart into the bulk solution quickly. Fowler et al. [18] found that the bound Ca^{2+} ion will dissociate during their MD simulations of NaK with two K^+ ions initially bound at site S4 and the cavity, respectively. It may be due to the larger fluctuation of the selectivity filter in such initial configuration of ions, as ion binding states are essential to structure stability of the selectivity filter [6,8]. As a result, structure stability of the selectivity filter may also influence the Ca^{2+} binding properties.

Table 2
Comparison of coordination and hydration numbers for the ions in the selectivity filter

Configuration	Ca_K		K1		K2		Ca_{Na}		Na1		Na2	
	n_c	n_h	n_c	n_h	n_c	n_h	n_c	n_h	n_c	n_h	n_c	n_h
C13	8.0	4.0	5.9	1.0	8.2	0.9	8.0	4.0	5.7	1.3	5.7	1.3
C14	8.0	4.0	6.0	1.4	7.2	4.1	6.8	6.3	5.8	2.0	6.0	3.9
C23	8.0	4.0	7.2	2.0	7.9	1.1	8.0	4.0	6.0	2.0	5.9	3.3
C24	8.0	4.0	6.7	1.8	7.0	5.8	8.0	4.0	5.5	3.4	5.9	3.8
C34	8.0	4.0	6.7	2.0	8.0	1.1	8.0	4.0	6.0	2.0	5.6	4.3

Ca_K and Ca_{Na} are the Ca^{2+} ions at site Sext in the K^+ and Na^+ simulations, respectively. K1, K2 and Na1, Na2 are the K^+ and Na^+ ions in the selectivity filter numbered from the extracellular to the intracellular sides. n_c and n_h are the coordination number and hydration number, respectively. The coordination number and hydration number are calculated by integrating over the ion–oxygen and ion–water oxygen radial distribution functions (RDFs), respectively, up to a radial cutoff of 3.6 Å for K^+, 3.2 Å for Na^+ and 3.2 for Ca^{2+}.

3.3. Solvation states for the ions in the selectivity filter

To study the dynamic interactions among the ions, water molecules and the channel protein, we calculated ion–oxygen radial distribution functions and coordination numbers, together with ion–water oxygen radial distribution functions and hydration numbers, for the K^+ and Na^+ ions in the selectivity filter and the Ca^{2+} ion at site Sext (Fig. 6), as performed by Noskov et al. [14,15]. In our simulations, the ion parameters are adjusted to accurately represent the interactions of ions with water and the protein according to [27]. The adjusted parameters have been shown to be able to generate reasonable ionic

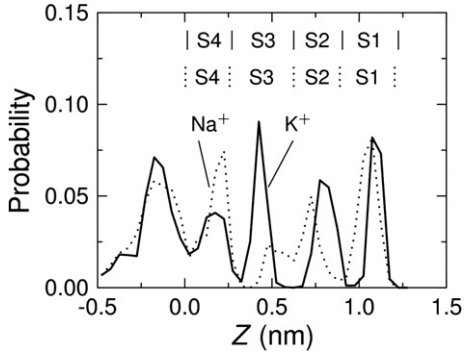

Fig. 4. Probability distributions of the Z positions of the K^+ (solid line) and Na^+ (dotted line) ions in the pore. Vertical lines indicate the mean Z positions of the oxygen atoms of the filter averaged over the four subunits. The results were obtained from all the simulation trajectories with initial configurations C13, C14, C23, and C24.

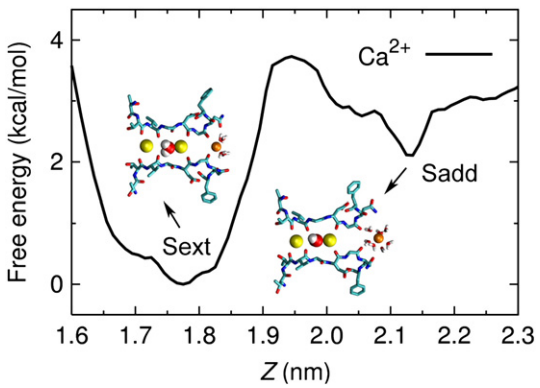

Fig. 5. One-dimensional potential of mean force as a function of the position of the Ca^{2+} ion, while the two K^+ ions bind at sites S1 and S3, respectively.

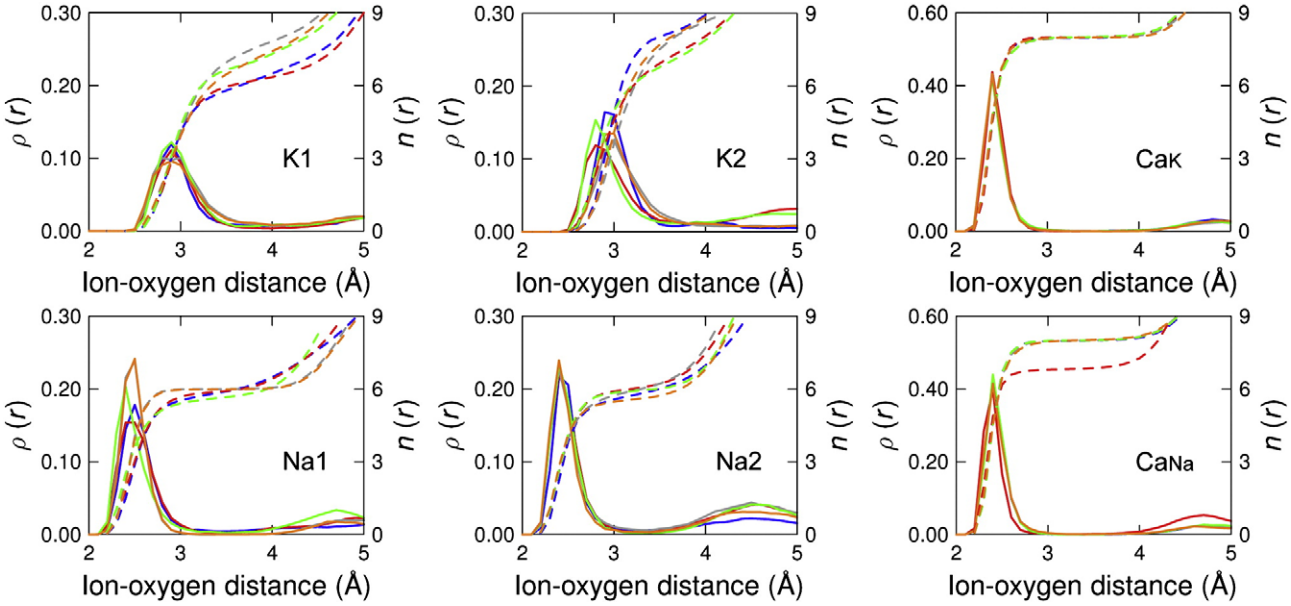

Fig. 6. Radial distribution function $\rho(r)$ (solid line) and coordination number $n(r)$ (dashed line) for the K^+ and Na^+ ions in the selectivity filter and the Ca^{2+} ion at site Sext in simulations with different initial configurations: C13 (blue), C14 (red), C23 (gray), C24 (green) and C34 (orange).

solvation states [19,35]. The results for K^+ differ strikingly from that for Na^+. Compared to Na^+, the first peak is lower, the first minimum is higher and their corresponding positions are more diverse for K^+. The positions of the first peak and the first minimum are in the range of 2.8–3.0 and 3.7–4.2 Å, respectively, for K^+, while they are in the range of 2.4–2.5 and 3.2–3.5 Å, respectively, for Na^+. It is also shown that the coordination number curve for Na^+ is lower and more flat than that for K^+ around the position of the first minimum. So that K^+ has a wider variety of coordination numbers. Coordination number and hydration number reflect the average number of ligands and water oxygen atoms falling within the first solvation shell of an ion, respectively [14,35,36]. For convenience, we use a fixed distance, 3.6 Å for K^+, 3.2 Å for Na^+ [34] and 3.2 Å for Ca^{2+} [37], as the outer limit of the first solvation shell, and the resulted coordination and hydration numbers for the ions are summarized in Table 2. At first sight, the fluctuation in the coordination numbers for the K^+ ions is wider than that for the Na^+ ions. The K^+ ions display different coordination numbers (5.9–8.2) over the selectivity filter, while the Na^+ ions have the coordination numbers concentrated at 6.0 with narrow scatter. Previous simulations with K^+ or Na^+ ion in the selectivity filter of NaK [15,18,20] or in bulk solution [19] showed similar coordination properties. It is suggested that both K^+ and Na^+ ions can achieve favorable solvation states during their conduction through the pore.

Analysis of the hydration numbers of the K^+ ions reveals that the K^+ ions binding at sites S1, S2, and S3 are hydrated approximately by one, two, and one water molecules, respectively; while the hydration numbers for the K^+ ions initially at site S4 are larger than 4.0, as shown in [18], and the Thr63 residues cannot coordinate the K^+ ion as good as the other residues lining the filter do. It may be due to the larger fluctuation of the side-chain of Thr63. The hydration property of Na^+ ions is more complex than that of K^+ ions. When a Na^+ ion diffuses in the vestibule, it can be hydrated by 1–4 water molecules moving in the vestibule–grottos complex. The Na^+ ion at site S4 is hydrated by ~4 water molecules. Site S23 is a preference site for Na^+ ion, where the Na^+ ion has a constant hydration number of two. Noskov and Roux [15] also reported that the ions in the selectivity filter of NaK are slightly more hydrated than in KcsA. Fowler et al. [18] have obtained similar results when the CHARMM force field is used.

3.4. Orientation of the carbonyl groups of the selectivity filter

Spontaneous reorientation of the carbonyl group of the selectivity filter, pointing alternatively towards and away from the pore, has been observed in previous MD simulations of KcsA [7,24], Kir6.2 [38], KirBac1.1 [39], Kv1.2 [40], and NaK [18]. It was suggested that the orientation of the carbonyl group can be influenced by ion binding states and the interactions between the residues of the filter and its adjacent pore helix [41]. Further analysis revealed that such a

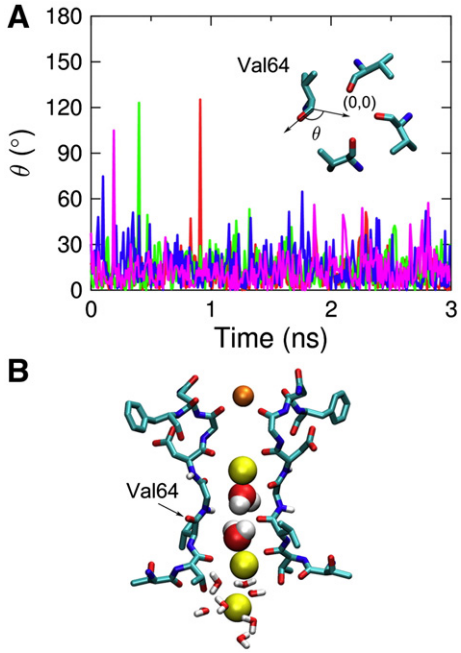

Fig. 7. Reorientation of the backbone carboxyl of Val64 for the K^+ simulation in configuration C14. (A) Angles projected in the *xy* plane between the CO vectors of residues Val64 of the four subunits and the corresponding C-origin vectors, as illustrated by the inset. (B) A snapshot of the selectivity filter showing the reorientation of the carbonyl of Val64 (as indicated by arrow) of one of the four subunits.

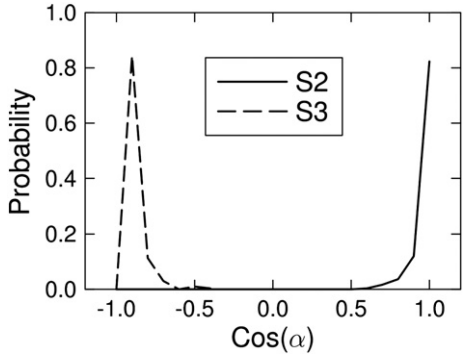

Fig. 8. Probability distributions of dipole orientations of water molecules at sites S2 and S3 for the K^+ simulation in configuration C14. α is the angle between a water dipole and the membrane normal.

spontaneous isomerization transition of Val76 in KcsA might be correlated with the translocation of the K^+ ions and water molecules [7,24], and channel gating [41]. Our simulations show that spontaneous reorientation of the carbonyl group of Val64, corresponding to Val76 in KcsA, only occurs in simulation C14/K^+ (Fig. 7B). The orientation variations of the four carbonyl groups of Val64 residues with time are drawn in Fig. 7A. Three large transient reorientation events are observed. More careful analysis of the trajectory of C14/K^+ shows that both the interactions of water molecules and ions with the carbonyl oxygen atoms of Val64 play an important role in preventing the transient reorientation of the carbonyl group. In simulation C14/K^+, both sites S2 and S3 are occupied by water molecules. Fig. 8 shows the probability distributions of dipole orientations of the two water molecules at sites S2 and S3. It can be seen that the two water molecules at sites S2 and S3 have an apparent preference for their dipole orientations along the Z and $-Z$ directions, respectively. As a consequence, they can form favorable hydrogen bonds with the four carbonyls of residues Val64, which in turn prevent the transient reorientation of the carbonyl group of Val64. Further analysis shows that water molecules in the vestibule are all ordered with their oxygen

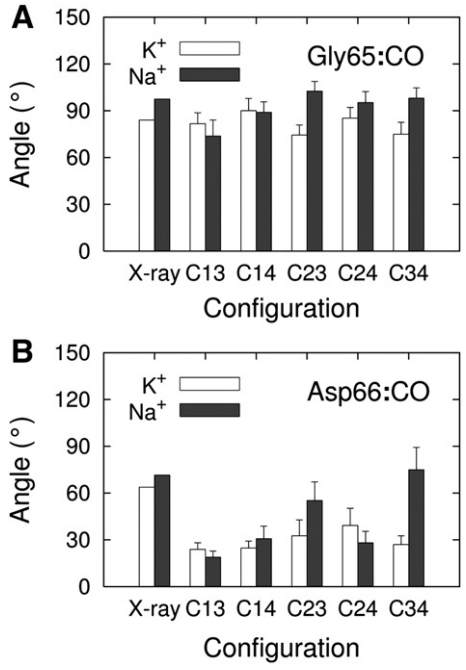

Fig. 9. Comparison of the carbonyl groups orientations of (A) Gly65, and (B) Asp66 in crystal structures and simulations with K^+ (empty) or Na^+ (gray) ions in the pore. Results (mean ± s.d.) were calculated during the last 2 ns in each simulation and averaged over the four subunits.

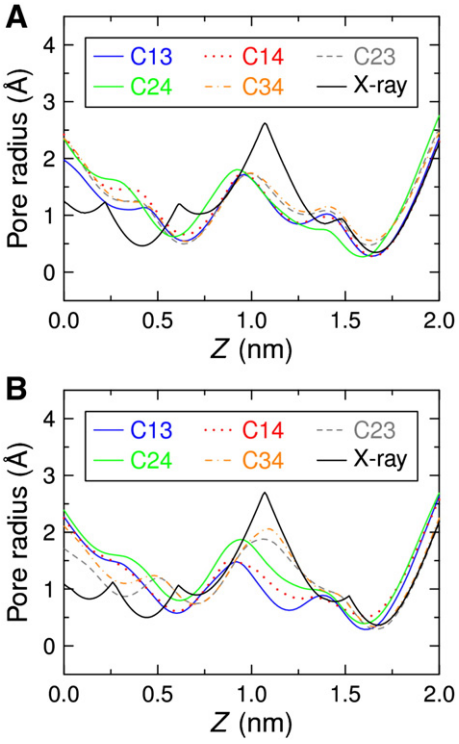

Fig. 10. Comparison of pore radius profiles for the selectivity filter in the crystal structure and MD simulations with (A) K^+ or (B) Na^+ ions in the pore. In each simulation, the pore radius profile was averaged over the whole 3 ns trajectory.

atoms pointing towards the hydrated ion. Orientations of the carbonyl groups of Gly65 and Asp66 in all of the simulations, as well as in the crystal structures, are also calculated for their correlation with the ion binding states (Fig. 9). As in the crystal structures, the carbonyl group of Gly65 aligns tangentially to the pore in all of the simulations, and there are no significant differences between different simulations. In contrast, the carbonyl group of Asp66 always reorients to point towards the pore except in simulations C23/Na^+ and C34/Na^+. It is suggested that the orientations of the carbonyl groups of Gly65 and Asp66 are the results of competition between ion–carbonyl/water–carbonyl attraction and carbonyl–carbonyl/water–carbonyl repulsion. The carbonyl groups of Asp66 will reorient to point towards the center pore if there is one ion in the vestibule.

Pore radius profiles calculated with HOLE [42] for the selectivity filter in different simulations are compared with that of the crystal structures (Fig. 10). Expanding of the intracellular entrance to the selectivity filter is observed in all of the simulations, similar to previous MD simulations of Kir6.2 [38] and NaK [18]. It may be due to the large thermal fluctuations of the side-chain atoms of residues Thr63 and the low ion binding affinity at site S4. Shrinking of the vestibule is another notable difference between the simulations and the crystal structures. It is consistent with the orientations of the carbonyl groups of the filter discussed above. Reorientation of the carbonyl group of Asp66 is the main reason for vestibule shrinking.

4. Conclusions

In this study, we carried out extensive MD simulations of the NaK channel with different initial configurations of ions (pure K^+ or Na^+) and water molecules in the pore. Examination of the MD trajectories indicates that K^+ ions and Na^+ ions exhibit different binding states in the selectivity filter, and their stable configurations in the NaK channel are also different from that in KcsA. In the NaK channel, K^+ ion prefers to sit at site S3, whereas Na^+ ion favors to bind at site S23. It is observed that simulations with K^+ or Na^+ ion at site S3 or S23

have the lowest backbone RMSDs of the selectivity filter. In K^+ simulations, K^+ ions can occupy two adjacent sites, S2 and S3 simultaneously, or be separated by two water molecules. While in KcsA, the configurations with two ions separated by one water molecule are the stablest. Previous MD simulations of NaK without Ca^{2+} blockage have shown that it is necessary to have an ion binding at S1 to maintain the stability of the selectivity filter. It indicates that the Ca^{2+} ion not only stabilizes the filter but also changes the ions distributions in the selectivity filter. Furthermore, ions can diffuse within the vestibule hydrated by water molecules confined within the vestibule–grottos complex. This coincides with a previous experimental report. It is also shown that a Ca^{2+} ion can bind at the half-dehydrated site Sext, or as in case of C14/Na^+, raise to a higher binding site Sadd in a fully hydrated state.

Both experimental [1] and computational [20] studies show that the NaK channel can conduct both K^+ and Na^+ ions, with a slight preference for the former, although it is still a challenge to deduce the K^+/Na^+ selectivity ratio at physiological condition [3,20]. Noskov and Roux [15] analyzed the selectivity of the NaK channel using free energy perturbation MD simulations, and they pointed out that the loss of the selectivity of the site S2, which is the most selective binding site in KcsA, contributes mainly to the lack of selectivity of NaK. Further calculations show that increased partial hydration of the ions in the selectivity filter of NaK is responsible for the loss of selectivity, which coincides with previous results of free energy calculations by Noskov et al. [14] that modifying the number and/or the type of the ligands coordinating the bound ion will change the selectivity of a flexible structure. Bostick and Brooks III [19], however, attribute the lack of selectivity to the loss of the constraint on the ions' coordination number by a population analysis of hydrated cations. Recent quantum-mechanical calculations [34,43] of simplified models consisting of an ion surrounded by various molecules also report that an eightfold coordinated site is always K^+-selective, and a decrease in the coordination number will cause a loss of the selectivity for K^+. Our analyses of the coordination and hydration numbers of the ions in the selectivity filter reveal that the fluctuation in the coordination number for Na^+ is less than that for K^+. Over the selectivity filter, Na^+ has a stable coordination number very close to 6, while K^+ ion displays a broader range of coordination number (5.9–8.2). The existent of the vestibule and the water molecules in the vestibule–grottos complex play an important part in the attainment of favorable coordination states for both K^+ and Na^+ ions in the filter, which may result in the lack of K^+ selectivity of NaK. Recently, Alam and Jiang [44, 45] reported high-resolution structures of the open NaK channel. It is shown that the regions around the selectivity filter are essentially unaffected during the channel gating process. In agreement with our results, they presented that Na^+ ions tend to bind in plane with four carbonyl or hydroxyl oxygen atoms of the selectivity filter, instead of binding at the middle of the ion binding sites as K^+ ions. In addition, four water molecules were also found in the vestibule of NaK to coordinate the ions, and it demonstrates that water molecules play an important role in ion selectivity and conduction in NaK.

Shrinking vestibule is observed due to the orientations of the carbonyl groups of the residues lining the selectivity filter. When there is one ion in the vestibule, the Asp66 carbonyl group reorients to point towards the center pore, while the Gly65 carbonyl group has similar orientation as reported in the crystal structures. In addition, transient reorientation of the Val64 carbonyl group can infrequently be observed, similar to that in KcsA.

Acknowledgments

The work is supported by 973 Program (2007CB936204), the Ministry of Education (No. 705021, IRT0534) and National NSF (10732040) of China.

References

[1] N. Shi, S. Ye, A. Alam, L. Chen, Y. Jiang, Atomic structure of a Na^+- and K^+-conducting channel, Nature 440 (2006) 570–574.
[2] W.N. Zagotta, Membrane biology: permutations of permeability, Nature 440 (2006) 427–429.
[3] A. Alam, N. Shi, Y. Jiang, Structural insight into Ca^{2+} specificity in tetrameric cation channels, Proc. Natl. Acad. Sci. U. S. A. 104 (2007) 15334–15339.
[4] U.B. Kaupp, R. Seifert, Cyclic nucleotide-gated ion channels, Physiol. Rev. 82 (2002) 769–824.
[5] D.A. Doyle, J.H. Morais-Cabral, R.A. Pfuetzner, A. Kuo, J.M. Gulbis, S.L. Cohen, B.T. Chait, R. MacKinnon, The structure of the potassium channel: molecular basis of K^+ conduction and selectivity, Science 280 (1998) 69–77.
[6] Y. Zhou, J.H. Morais-Cabral, A. Kaufman, R. MacKinnon, Chemistry of ion coordination and hydration revealed by a K^+ channel–Fab complex at 2.0 Å resolution, Nature 414 (2001) 43–48.
[7] C. Domene, M.S.P. Sansom, Potassium channel, ions, and water: simulation studies based on the high resolution X-ray structure of KcsA, Biophys. J. 85 (2003) 2787–2800.
[8] J.H. Morais-Cabral, Y. Zhou, R. MacKinnon, Energetic optimization of ion conduction rate by the K^+ selectivity filter, Nature 414 (2001) 37–42.
[9] J. Aqvist, V. Luzhkov, Ion permeation mechanism of the potassium channel, Nature 404 (2000) 881–884.
[10] S. Berneche, B. Roux, Energetics of ion conduction through the K^+ channel, Nature 414 (2001) 73–77.
[11] M. Zhou, R. MacKinnon, A mutant KcsA K^+ channel with altered conduction properties and selectivity filter ion distribution, J. Mol. Biol. 338 (2004) 839–846.
[12] I.H. Shrivastava, M.S.P. Sansom, Simulations of ion permeation through a potassium channel: molecular dynamics of KcsA in a phospholipid bilayer, Biophys. J. 78 (2000) 557–570.
[13] I.H. Shrivastava, D.P. Tieleman, P.C. Biggin, M.S.P. Sansom, K^+ versus Na^+ ions in a K channel selectivity filter: a simulation study, Biophys. J. 83 (2002) 633–645.
[14] S.Y. Noskov, S. Berneche, B. Roux, Control of ion selectivity in potassium channels by electrostatic and dynamic properties of carbonyl ligand, Nature 431 (2004) 830–834.
[15] S.Y. Noskov, B. Roux, Importance of hydration and dynamics on the selectivity of the KcsA and NaK channels, J. Gen. Physiol. 129 (2007) 135–143.
[16] A.D. MacKerell Jr., D. Bashford, M. Bellott, R.L. Dunbrack Jr., J.D. Evanseck, M.J. Field, S. Fischer, J. Gao, H. Guo, S. Ha, D. Joseph-McCarthy, L. Kuchnir, K. Kuczera, F.T.K. Lau, C. Mattos, S. Michnick, T. Ngo, D.T. Nguyen, B. Prodhom, W.E. Reiher III, B. Roux, M. Schlenkrich, J.C. Smith, R. Stote, J. Straub, M. Watanabe, J. Wiorkiewicz-Kuczera, D. Yin, M. Karplus, All-atom empirical potential for molecular modeling and dynamics studies of proteins, J. Phys. Chem. B 102 (1998) 3586–3616.
[17] W.D. Cornell, P. Cieplak, C.I. Bayly, I.R. Gould, K.M. Merz Jr., D.M. Ferguson, D.C. Spellmeyer, T. Fox, J.W. Caldwell, P.A. Kollman, A second generation force field for the simulation of proteins and nucleic acids, J. Am. Chem. Soc. 117 (1995) 5179–5197.
[18] P.W. Fowler, K. Tai, M.S.P. Sansom, The selectivity of K^+ ion channels: testing the hypotheses, Biophys. J. 95 (2008) 5062–5072.
[19] D.L. Bostick, C.L. Brooks III, Selectivity in K^+ channels is due to topological control of the permeant ion's coordinated state, Proc. Natl. Acad. Sci. U. S. A. 104 (2007) 9260–9265.
[20] T. Vora, D. Bisset, S.H. Chung, Conduction of Na^+ and K^+ through the NaK channel: molecular and Brownian dynamics studies, Biophys. J. 95 (2008) 1600–1611.
[21] W. Humphrey, A. Dalke, K. Schulten, Vmd: visual molecular dynamics, J. Mol. Graph. 14 (1996) 33–38.
[22] Y. Wang, K. Schulten, E. Tajkhorshid, What makes an aquaporin a glycerol channel? A comparative study of AqpZ and GlpF, Structure 13 (2005) 1107–1118.
[23] W.Y. Zhong, W.L. Guo, S.J. Ma, Intrinsic aqueduct orifices facilitate K^+ channel gating, FEBS Lett. 582 (2008) 3320–3324.
[24] S. Berneche, B. Roux, Molecular dynamics of the KcsA K^+ channel in a bilayer membrane, Biophys. J. 78 (2000) 2900–2917.
[25] J.C. Phillips, R. Braun, W. Wang, J. Gumbart, E. Tajkhorshid, E. Villa, C. Chipot, R.D. Skeel, L. Kale, K. Schulten, Scalable molecular dynamics with NAMD, J. Comput. Chem. 26 (2005) 1781–1802.
[26] W.L. Jorgensen, J. Chandrasekhar, J.D. Madura, R.W. Impey, M.L. Klein, Comparison of simple potential functions for simulating liquid water, J. Chem. Phys. 79 (1983) 926–935.
[27] B. Roux, S. Berneche, On the potential functions used in molecular dynamics simulations of ion channels, Biophys. J. 82 (2002) 1681–1684.
[28] U. Essmann, L. Perera, M.L. Berkowitz, T. Darden, H. Lee, L.G. Pedersen, A smooth particle mesh Ewald method, J. Chem. Phys. 103 (1995) 8577–8593.
[29] S.E. Feller, Y. Zhang, R.W. Pastor, B.R. Brooks, Constant pressure molecular dynamics simulation: the Langevin piston method, J. Chem. Phys. 103 (1995) 4613–4621.
[30] G.J. Martyna, D.J. Tobias, M.L. Klein, Constant pressure molecular dynamics algorithms, J. Chem. Phys. 101 (1994) 4177–4189.
[31] G.M. Torrie, J.P. Valleau, Nonphysical sampling distributions in Monte Carlo free-energy estimation: umbrella sampling, J. Comput. Phys. 23 (1977) 187–199.
[32] S. Kumar, D. Bouzida, R.H. Swendsen, P.A. Kollman, J.M. Rosenberg, The weighted histogram analysis method for free-energy calculations on biomolecules. I. The method, J. Comput. Chem. 13 (1992) 1011–1021.
[33] C.E. Capener, I.H. Shrivastava, K.M. Ranatunga, L.R. Forrest, G.R. Smith, M.S.P. Sansom, Homology modeling and molecular dynamics simulation studies of an inward rectifier potassium channel, Biophys. J. 78 (2000) 2929–2942.
[34] M. Thomas, D. Jayatilaka, B. Corry, The predominant role of coordination number in potassium channel selectivity, Biophys. J. 93 (2007) 2635–2643.

[35] A. Grossfield, P. Ren, J.W. Ponder, Ion solvation thermodynamics from simulation with a polarizable force field, J. Am. Chem. Soc. 125 (2003) 15671–15682.
[36] T.W. Allen, S. Kuyucak, S.H. Chung, Molecular dynamics study of the KcsA potassium channel, Biophys. J. 77 (1999) 2502–2516.
[37] D. Jiao, C. King, A. Grossfield, T.A. Darden, P.Y. Ren, Simulation of Ca^{2+} and Mg^{2+} solvation using polarizable atomic multipole potential, J. Phys. Chem. B 110 (2006) 18553–18559.
[38] C.E. Capener, P. Proks, F.M. Ashcroft, M.S.P. Sansom, Filter flexibility in a mammalian K channel: models and simulations of Kir6.2 mutants, Biophys. J. 84 (2003) 2345–2356.
[39] C. Domene, A. Grottesi, M.S.P. Sansom, Filter flexibility and distortion in a bacterial inward rectifier K^+ channel: simulation studies of KirBac1.1, Biophys. J. 87 (2004) 256–267.
[40] F. Khalili-Araghi, E. Tajkhorshid, K. Schulten, Dynamics of K^+ ion conduction through Kv1.2, Biophys. J. 91 (2006) L72–L74.
[41] S. Berneche, B. Roux, A gate in the selectivity filter of potassium channels, Structure 13 (2005) 591–600.
[42] O.S. Smart, J.M. Goodfellow, B.A. Wallace, The pore dimensions of gramicidin A, Biophys. J. 65 (1993) 2455–2460.
[43] S. Varma, S.B. Rempe, Tuning ion coordination architectures to enable selective partitioning, Biophys. J. 93 (2007) 1093–1099.
[44] A. Alam, Y. Jiang, High-resolution structure of the open NaK channel, Nat. Struct. Mol. Biol. 16 (2009) 30–34.
[45] A. Alam, Y. Jiang, Structural analysis of ion selectivity in the NaK channel, Nat. Struct. Mol. Biol. 16 (2009) 35–41.